Taylor & Francis
Taylor & Francis Group

Expert Opinion on Therapeutic Patents

ISSN: (Print) (Online) Journal homepage: www.tandfonline.com/journals/ietp20

CBL-B – An upcoming immune-oncology target

Riccardo Fusco, Zeinab Saedi, Imma Capriello, Andriy Lubskyy & Alexander Dömling

To cite this article: Riccardo Fusco, Zeinab Saedi, Imma Capriello, Andriy Lubskyy & Alexander Dömling (2025) CBL-B – An upcoming immune-oncology target, Expert Opinion on Therapeutic Patents, 35:1, 47-64, DOI: 10.1080/13543776.2024.2412567

To link to this article: https://doi.org/10.1080/13543776.2024.2412567

Published online: 25 Nov 2024.

EXPERT OPINION ON THERAPEUTIC PATENTS
2025, VOL. 35, NO. 1, 47–64
https://doi.org/10.1080/13543776.2024.2412567

Taylor & Francis
Taylor & Francis Group

REVIEW

OPEN ACCESS Check for updates

CBL-B – An upcoming immune-oncology target

Riccardo Fusco[a,b], Zeinab Saedi[a,b], Imma Capriello[a,b], Andriy Lubskyy[a,b] and Alexander Dömling [a,b]

[a]Institute of Molecular and Translational Medicine, Faculty of Medicine and Dentistry, Palacky University, Olomouc, Czechia; [b]Czech Advanced Technology and Research Institute, Palacky University, Olomouc, Czechia

ABSTRACT

Introduction: The E3 ubiquitin ligase Cbl-b is a novel target in immune-oncology, with critical roles in regulating T-cell activation and signaling pathways. By facilitating the ubiquitination and degradation of key signaling proteins, Cbl-b modulates immune responses, maintaining immune homeostasis and preventing unwarranted T-cell proliferation. The therapeutic potential of Cbl-b as a cancer immunotherapy target is underscored by its contribution to an immunosuppressive tumor microenvironment, with efforts currently underway to develop small-molecule inhibitors.

Areas covered: We reviewed the small molecules, and antibody-drug conjugates targeting Cbl-b from 2018 to 2024. The patents were gathered through publicly available databases and analyzed with in-house developed cheminformatic workflow, described within the manuscript.

Expert opinion: Targeting Cbl-b presents a promising approach in immuno-oncology, offering a novel pathway to potentiate the immune system's ability to combat cancer beyond PDL1/PD1 inhibition. The development and clinical advancement of Cbl-b inhibitors, as evidenced by the ongoing trials, mark a significant step toward harnessing this target for therapeutic benefits. Overall, the strategic inhibition of Cbl-b holds substantial promise for improving cancer immunotherapy outcomes, heralding a new era in the fight against cancer.

ARTICLE HISTORY
Received 22 May 2024
Accepted 1 October 2024

KEYWORDS
CBL-B; immune oncology; small molecule; antibody drug conjugate; automated patent analysis

1. Introduction

The E3 ubiquitin ligase Cbl-b (also termed RNF56) is a member of a highly conserved family of Cbl (casitas b-lineage lymphoma) proteins, which play a pivotal role as the negative regulators of T-cell activation, growth factor receptor, and nonreceptor-type tyrosine kinase signaling. Cbl proteins mediate ubiquitination and consequently proteasomal or, in some cases, lysosomal degradation of various signaling transducers, resulting in attenuation of the relevant signals [1]. Among Cbl proteins, Cbl-b, preferential expression in CD4+ and CD8+ T cells, plays a critical role in the down-regulation of immunological signaling to induce T-cell anergy [2].

Cbl-b, as an intracellular mediator, serves as a crucial link between CD28 and CTLA-4 receptor signaling (Figure 1). The receptor CD28 provides a secondary signal to activate T cells upon TCR/MHC-II binding. Following T cell activation, the expression of CTLA-4 increases to outcompete the binding of CD28 to its ligands, CD80 and CD86, which reduces the risk of unnecessary T cell proliferation in normal 'healthy' conditions. In the absence of CD28 co-stimulation, Cbl-b initiates the ubiquitination of crucial proteins such as PI3K, PLCγ, the zeta-subunit of TCR, and NEDD4, resulting in the prevention of Vav1-mediated cytoskeletal activation, TCR phosphorylation, and PTEN inactivation. Cbl-b also promotes TGF-ß signaling through the ubiquitination of SMAD7. Conversely, ubiquitination of Cbl-b and its subsequent lysosomal degradation occurs after a successful CD28 receptor co-stimulation, preventing an anergic response [3,4].

The inhibitory effect of Cbl-b promotes an immunosuppressive tumor environment, making it a potential therapeutic target for cancer immunotherapy besides immune-related disorders, such as infections and autoimmune diseases [5]. Several reports have shown that Cbl-b deficient animals reject tumors in various autochthonous and transplanted tumor models [6–8]. As a well-established and significant immune checkpoint, no approved drug for inhibiting Cbl-b is currently on the market. Nonetheless, at present, two small molecules of Cbl-b inhibitors, HST-1011 (ClinicalTrials.gov ID: NCT05662397) and Nx-1607 (ClinicalTrials.gov ID: NCT05107674), are in the clinical trials by HotSpot and Nurix, respectively. Several biology and chemistry-centric reviews were recently published [2,5,9,10]. In the present review, we focus on summarizing patents and literature of Cbl-b small-molecule inhibitors until January 2024.

1.1. Structural biology information

Cbl-b, consisting of 982 amino acid residues, has a highly conserved N-terminal region, including a tyrosine-kinase-binding domain (TKB) composed of a 4-helix bundle (4 h), a calcium-binding EF domain, and a variant SH2 domain. These three domains form an integrated phosphoprotein-recognition module [11]. A short linker-helix region (LHR)

CONTACT Alexander Dömling alexander.domling@upol.cz Institute of Molecular and Translational Medicine, Faculty of Medicine and Dentistry, Palacky University, Hněvotínská 1333/5, Olomouc 77900, Czech Republic

Article highlights

- This review covers the patents featuring Cbl-b targeting small-molecule inhibitors and antibody-drug conjugated disclosed up to January 2024.
- Cbl-b is a E3 ubiquitin ligase that mediates ubiquitination and degradation of various signaling inducers.
- Cbl-b promotes immunosuppressive tumor environment, making it a promising immune checkpoint target in cancer treatment.
- The binding target is well described, making for straightforward structure-based drug design.
- 2 compounds, NRX-1607 and HST-1011, are undergoing clinical trials at the date of manuscript publication.
- Data from patents was analyzed with help of in-house developed cheminformatic workflow based on open source and/or publicly available software.

connects the N-terminal region to a central RING finger domain, which binds the E2 conjugating enzyme and mediates the transfer of ubiquitin between E2 and target substrates [12]. The COOH-terminal region contains multiple proline-rich sequences, serine and tyrosine phosphorylation sites, and a ubiquitin-associated domain (UBA), which interacts with ubiquitin [13]. It has been shown that the phosphorylation of Tyr363, located in the LHR, eliminates Cbl-b autoinhibition and induces its ligation activity. The mutation of this highly conserved Tyr residue to Phe eliminates the E3 activity of Cbl-b [12].

In 2011, Kobashigawa et al. reported the structural analysis of the N-terminal region of Cbl-b both in the unphosphorylated and Tyr363-phosphorylated states using small-angle X-ray scattering (SAXS) and NMR spectroscopy (PDB ID: 3VGO). Their results revealed that Cbl-b has a compact structure in the unphosphorylated state due to an interaction between the TKB domain and several residues within the linker-helix region, especially Tyr363. In this compact conformation, the RING finger domain is restricted to the side of the TKB domain, and its interaction surface with the E2 ubiquitin-conjugating enzyme is completely masked. The phosphorylation of Tyr363 regulates the E3 activity of Cbl-b by disrupting the mentioned interdomain interaction to remove the masking of the RING domain from the TKB domain. Additionally, the phosphate group of phosphorylated Tyr363 is situated near the interaction surface with UbcH5B, resulting in a reduction of their electrostatic repulsion and, consequently, an increase in affinity [14].

Dou et al. have determined the crystal structure of phosphoTyr363-Cbl-b bound to a ZAP-70 substrate peptide and a Ub-linked E2 complex to investigate how monomeric RING E3s promote Ub transfer (PDB ID: 3ZNI). Their data indicate that both the pTyr363-induced structural element and pTyr363's direct interaction with Ub are required for positioning Ub for catalysis and improving the catalytic efficiency of Ub transfer by ~200-fold [15].

The identification of Cbl-b as a promising therapeutic target led to the discovery of multiple small-molecule inhibitors (Figure 2(a)), both from academia and industry. Published literature includes several co-crystal structures of these inhibitors with Cbl-b (PDB-IDs 8GCY,8QTK,8QTJ,8QTG,8QNG,8QNI,8QTH,8QNH). A comparative analysis of the co-crystallized Cbl-b structures has led to the formulation of a consensus pharmacophore model (Figure 2(b)). Based on the analysis of the crystal structure (Figure 2(c)) three primary pharmacophoric interactions critical for inhibitor efficacy: a solvent-exposed amine that engages Glu268 through electrostatic interactions (Figure 2(d)); the encapsulation of the central isoindolone substructure by surrounding amino acids (Figure 2(e)); and a hydrophobic channel that accommodates the 3-methyl cyclo-butane moiety, with

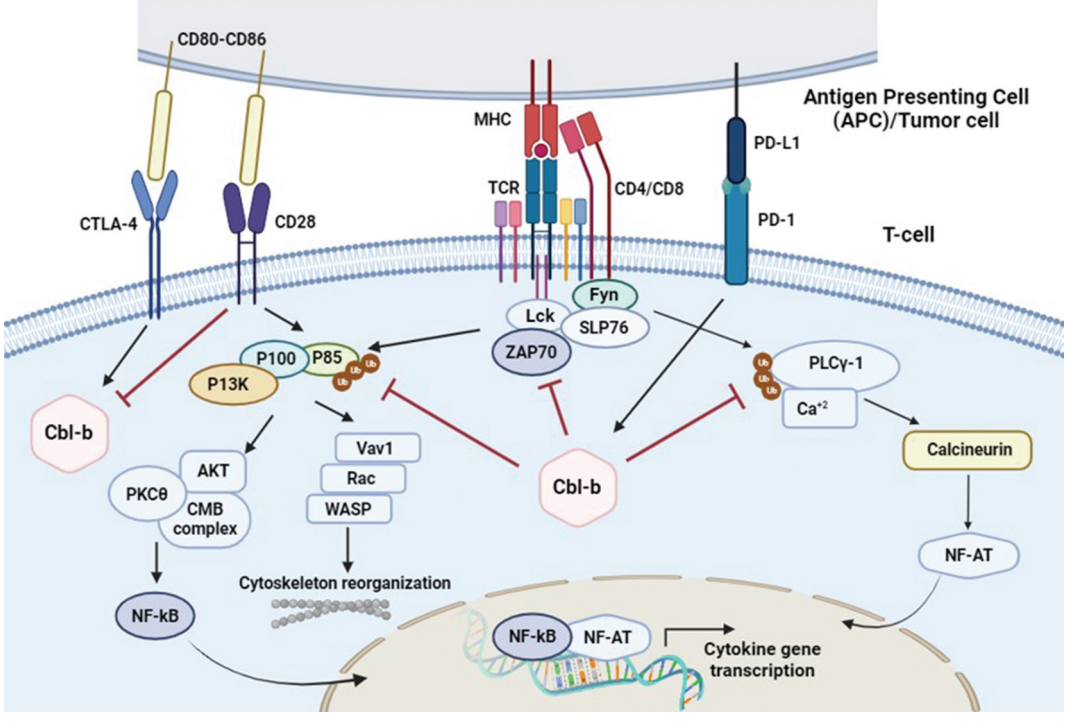

Figure 1. Involvement of Cbl-b in different pathways as the critical regulator of T-cell activation.

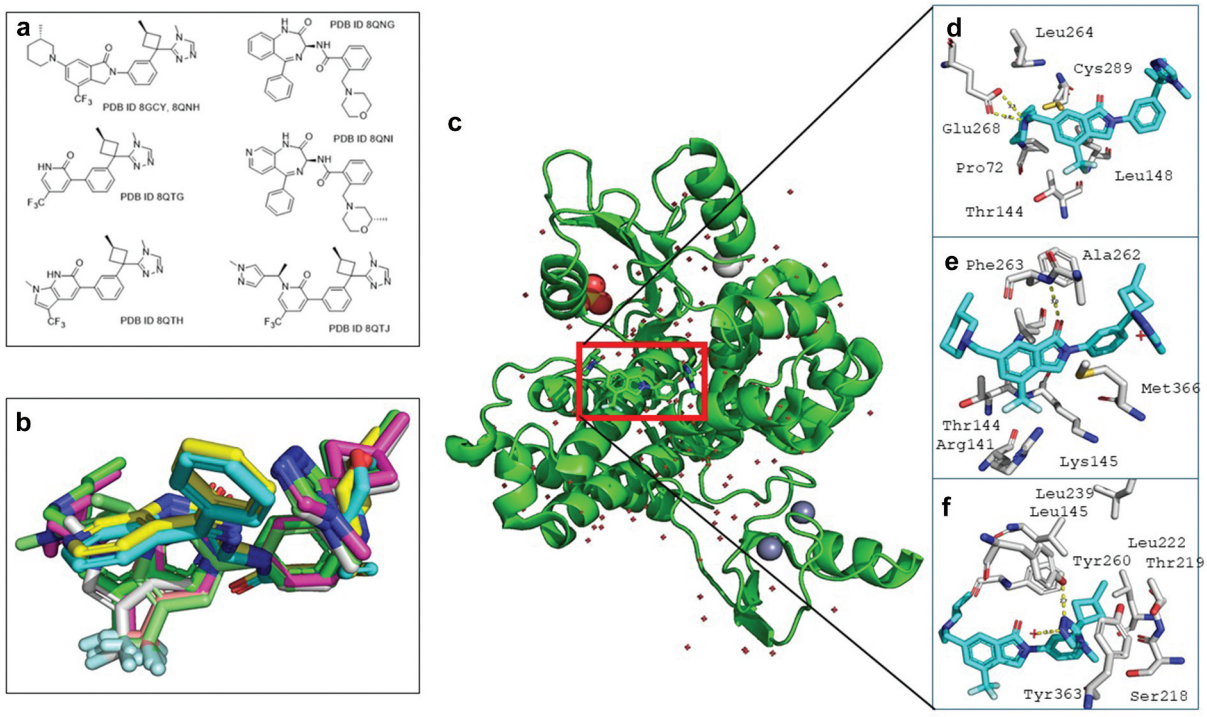

Figure 2. Structural biology information of Cbl-b small molecule interactions. a) 2D structures of the co-crystallized small molecules; b) Alignment of all small molecules of the co-crystallized Cbl-b structures supporting a common pharmacophore model; c) Overview of Cbl-b protein structure (PDB-ID 8GCY); d-f) Zoom into the small molecule binding site of the isoindolone structure partitioned into the three pharmacophore substructures; d) The solvent exposed amine binding site governed by a charge–charge interaction with Glu268 indicated as yellow dotted lines; e) The amino acids enclosing the central isoindolone substructure; f) A hydrophobic channel enclosing the 3-methyl cyclo-butane moiety; a triazole-N(3) forms a hydrogen bond to the Tyr260-oh and triazole-N(4) hydrogen bond to a water which is repeatedly involved in a H_2O cluster.

notable hydrogen bonds between triazole nitrogens and both Tyr260-OH and a water molecule within an H_2O cluster (Figure 2(f)).

2. Patent review

The patent review is ordered according to companies and patent priority dates.

2.1. Nurix therapeutics

Nurix Therapeutics has filed five patents featuring Cbl-b inhibitors in 2019–2022 [16–20] that were publicly disclosed in the following years. One of the patented compounds, NX-1607 (structure undisclosed), is currently undergoing a phase 1a clinical trial as an immune-oncology therapeutic agent (ID NCT05107674). Through all five patents, binding affinities of the disclosed small molecules were evaluated with Surface Plasmon Resonance (SPR), Fluorescence Resonance Energy Transfer (FRET) assays, and displacement assays and disclosed as ranges of IC_{50}. The T-Cell IL-2 secretion and CD25 surface expression were used for the evaluation of the biological activity of some compounds. Selected compounds were tested for T-cell, NK cell, and B-cell activities *in vivo* mouse models.

The first patent disclosed in 2019 features a fused benzo lactam (isoindoline-1-one) scaffold (General Structure 1), with the key pharmacophoric interaction being represented by the Hydrogen Bond between the lactam's carbonyl group and the backbone of the Phe263 (Figure 2(e)) [16]. The scaffold is joined through a (hetero) benzene linker to the pharmacophoric part of the molecule, consisting of an alkyl component (that includes the R_2 and R_3 group) and a triazole, as well as heterogeneous substitution on the A part of the molecule. The nature of an alkyl moiety R_2/R_3 did not substantially affect the IC_{50} – for example, compounds 1 and 2 both have the same IC_{50} range of 500 nM.

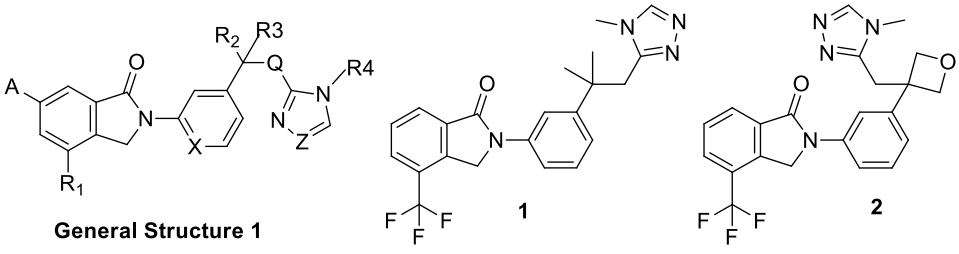

Various structures with 6-member aromatic linkers, such as phenyl and pyridyl, were also disclosed. Many different heterocyclic substituents were explored in A, including piperidine, morpholine, and more complex heterocycles such as naphthyridine, quinuclidine, and diazabicyclooctane. The molecules with an azaspiroheptane moiety showed the lowest IC_{50}, like 3 and 4 with IC_{50} less than 100 nM. The triazole group is notably prevalent across most of the disclosed structures. Chemists also explored an oxadiazole variant but observed no difference in activity. This likely occurred because both cases feature a nitrogen capable of forming a water bridge with the crystal water present in the subpocket around Tyr363.

A typical example of a compound disclosed in the patent is 5 (IC_{50} 5 μM), which usually has a 4-member ring at the R2-R3 position – replacing it with the 5-member ring oxolane results in compound 6 with an IC_{50} of over 100 μM. Interestingly, in the instances where a 4-membered ring has a chiral center, no significant difference in activity was observed between R and S configurations or among the various substitutions, like in compounds 7 and 8 (IC_{50} 5 μM).

Generally, adding piperazine in the A position tends to enhance the activity significantly, often tenfold. This is demonstrated by the difference in activity between 9 (IC_{50} 5 μM) and 10 (IC_{50} 12 μM). The presence of minor substitutions at the

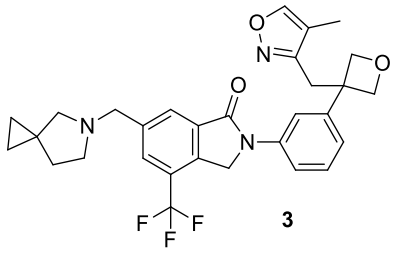

3

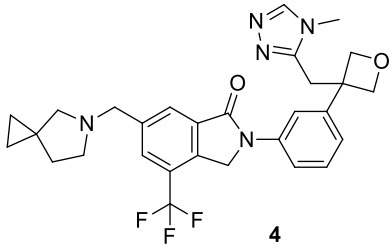

4

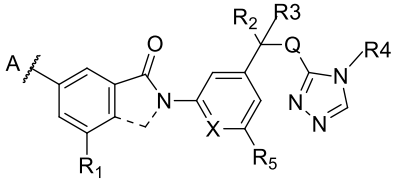

General Structure 2

The following three patents [17–19] were disclosed in 2020. They feature compounds with two central scaffolds: one benzamide and the cyclized isoindolin-1-one version (General Structure 2), and hence, they will be discussed together. All the compounds exhibit a broad range of activities up to 50 μM, independent of the central scaffold structure.

3-position of the piperidine ring helped improve the activity, demonstrated by 11 (IC_{50} 1 μM). However, adding a bigger or additional substituent is deleterious, widely decreasing the activity (12 and 13, 50 μM). Additional substitutions in other areas of the piperidine did not strongly affect the IC_{50} (14, 5.0 μM), thus making these substitutions a useful tool for adjusting the pharmacokinetic values.

Below are several notable examples that feature substituted pyridine attached to an isoindolin-1-one core. An additional ortho substituent can influence the compound's activity. For example, the binding affinity of 15 (IC_{50} of 1 μM) with an ethoxy moiety is much higher than that of 16 (IC_{50} – 50 μM) with a choline moiety.

In the last patent disclosed by Nurix, the chemists introduced a urea linker instead of the amide or lactam linker (General Structure 3) [20].

They further explored the A portion of the molecule from earlier patents, experimenting with various moieties such as

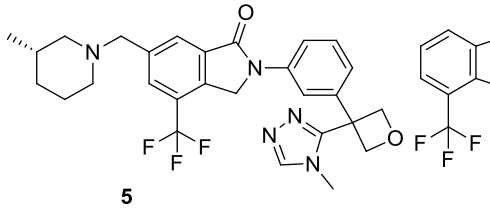

5

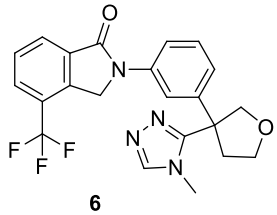

6

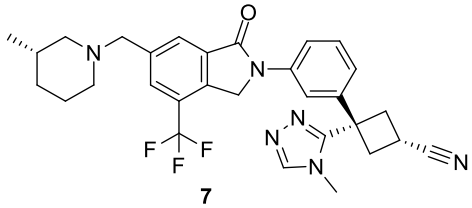

7

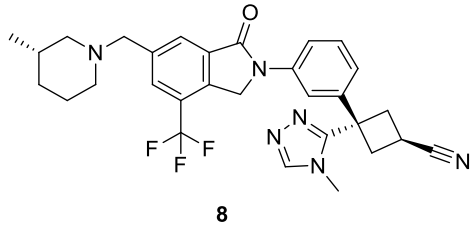

8

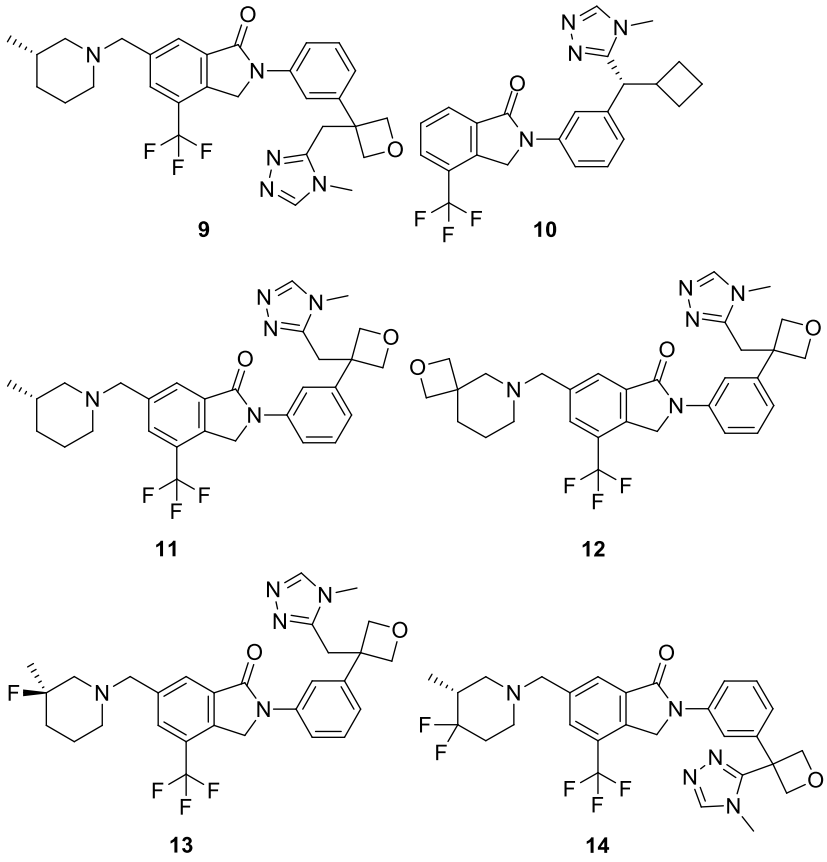

pyridoxazine (17, IC_{50} 5 μM) and a pyridine condensed morpholine spiro substituted. A notable example is 18, featuring a complex condensed morpholino pyridine cycle that exhibits an activity of 100 nM. This heightened activity is likely due to optimal interaction with the accessory subpocket (Figure 2(f)). Another intriguing example is 19 (IC_{50} 100 nM), which shed the phenyl-urea linker for a pyrazolopyridine core that interacts with Phe263 (Figure 2(e)) through the appropriate hydrogen atom.

2.2. Genentech

Genentech has released three patents [21–23] detailing compounds that exhibit inhibitory activity against Cbl-b. These molecules are claimed to act as inhibitors of Cbl-b. The binding activity data for the compounds were disclosed as TR-FRET IC_{50} activities. The *in vitro* biological activity was tested with Jurkat T-Cell assay and disclosed as EC_{50} concentration.

The first patent was disclosed in 2022 [21]. The scaffold under examination is anilino benzamide, characterized by General structure 4.

Q is an aromatic five-membered ring containing at least one heteroatom, while the central rings are often benzene or pyridine. R_1 and R_2 frequently feature oxetane, while in R_3 and/or R_4 the presence of a halogen seems to be crucial. Finally, R5 experiences predominant substitution with a heterocycloalkyl group, such as cyclopentyloxy group or N-cyclopentyl group.

Compound 20 shows the best IC_{50} value, corresponding to 7,1 nM. Various analogues of this compound have been analyzed, revealing that when R3 and R4 are both hydrogens, like in structure 21, the potency is reduced (IC_{50} of 7,5 nM). Similarly, when in structure 22, the carbon linking the fluorine in R3 has an S configuration, the potency is diminished (IC_{50} of 11 nM). Regarding the four-membered ring, when it corresponds to an oxetane, the IC_{50} values measured tend to be

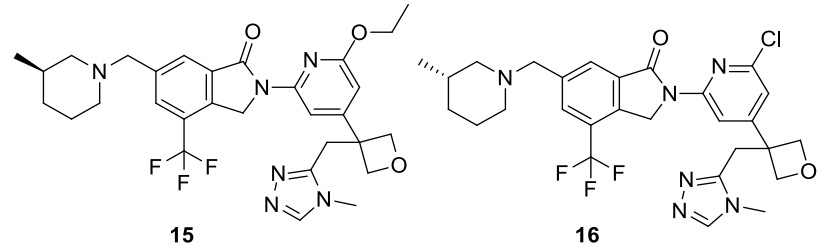

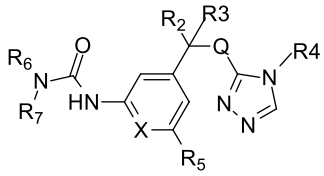

General Structure 3

higher. In structure 23, for example, showing an oxetane and two hydrogens in R3 and R4, the IC_{50} value is 10 nM.

Compound 24, instead, differs from the previously described compounds, because of the presence of a spirocyclic system substituted on the pyridine and because of the trifluoromethyl substituent. On the other hand, the complete absence of a third ring, as in compound 25, leads to a drastic decrease of the inhibitory activity (IC_{50} of 20 µM). This observation could be elucidated by the fact that the receptor pocket is not filled, as occurs when a third ring is present in the structure.

Interestingly, the oxygen atom in the oxetane ring is moved from the achiral position −3 to the chiral position −2: in compound 26, that shows a achiral oxetane moiety, the IC_{50} is 0.2 µM; in compound 27, where the oxetane oxygen instead changed position, the IC_{50} is 15 µM.

A second patent filed by Genentech was disclosed in 2023 and describes a group of γ-lactams, specifically the isoindoline-1-one core, summarized in general structure 5. [22]

Our analysis reveals similarities with the previously conducted study on the above anilino benzamides, suggesting that the g-lactams patent represents a progression or development of the one related to amides. Thus, similarities are observed in the substitutions in Q, R1, R2, R3, R4, and R5 positions. Z represents a versatile substitution pattern, taking the form of $-CH_2NR_7R_8$, where R_7 and R_8 are flexible and can be alkyl, cycloalkyl, heterocyclic, or spirocyclic groups. Furthermore, these substituents can be adorned with halogens, alkyl, cycloalkyl, and hydroxyalkyl groups. This substitution pattern allows for diverse modifications within the molecular scaffold.

In compound 28, R_1 and R_2 are oxetane, while R_3 and R_4 are two hydrogens, and Q is a 4-methyl-1,2,4-triazole. This combination is frequent, particularly in compounds with good inhibitory activity. In the case of compound 29, the IC_{50} value corresponds to 5,5 nM.

A cyano group is in R_5, such as in compound 30, is also tolerated, with the IC_{50} is 11 nM, so is an ethyleneamine group like in compound 31 with the IC_{50} is 12 nM. Nevertheless, as an interaction is likely occurring with a lipophilic sub-pocket of the receptor, the substitution in R_5 enhances the activity. In compound 32, a phenyl group in X significantly reduces the IC_{50} to a value higher than 20 µM.

The compound 33 is one of the most active compounds disclosed in the patent with an IC_{50} of 7 nM, incorporating a methyl substituent with an S stereocenter in the oxazepane moiety. When the same carbon shows an R configuration, like in compound 34, the IC_{50} increases considerably to 48 nM.

A third patent was disclosed in 2023 [23]. Once again, the compounds described are lactams with the isoindoline-1-one core and of General Structure 6.

The main distinguishing factor from the previously analyzed lactams is the absence of a carbon atom between the substituents R_3/R_4 and the Q ring, which results in a loss of a rotatable bond in this region and therefore increases the conformational rigidity. In **35**, the isoindoline-1-one scaffold is decorated with a cyclobutyl in R_3, with a methylene bridge to a cyano group. Q is a 4-methyl-1,2,4-triazole, while in R_1, a trifluoromethyl group is present. Finally, in Z, there is a 1-methylcyclobutylaminomethyl group. This combination leads to the best compound described in this patent, with an IC_{50} of 2,5 nM. On the other hand, what seems to decrease the compounds' inhibiting activity are the substitutions in J, like for compounds **36** (with a methoxy group, IC_{50} of 20 µM) and the difluoromethyl group in R_1 position, like in 37, with an IC_{50} of 9.9 µM.

2.3. HotSpot therapeutics

HotSpot Therapeutics filed a patent for Cbl-b inhibitors in 2021, which was published in 2022 [24]. The company's

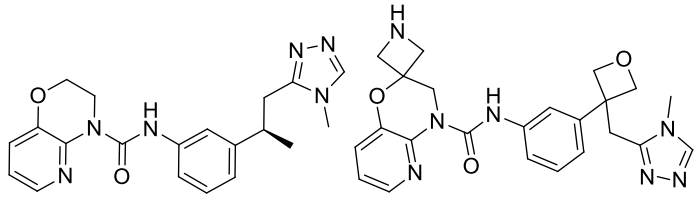

17 **18**

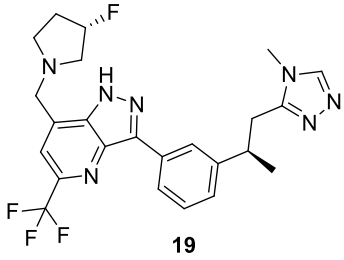

19

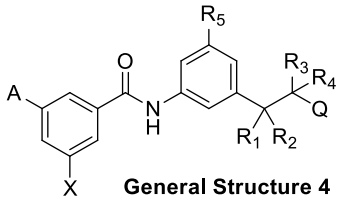

General Structure 4

small molecule, HST-1011 (structure undisclosed), is undergoing clinical trials (ClinicalTrials.gov ID: NCT05662397) for treating solid tumors. The patent showcases a series of structures of substituted imidazolo[1,5-a]pyridine-3(2 h)-ones, along with their corresponding TR-FRET activity data published as a range of IC_{50} values.

The general structure (General structure 7) of the active compounds in the patent consists of a heterocycle-benzene moiety that acts as a bridge between A (typically alkyl-triazole)

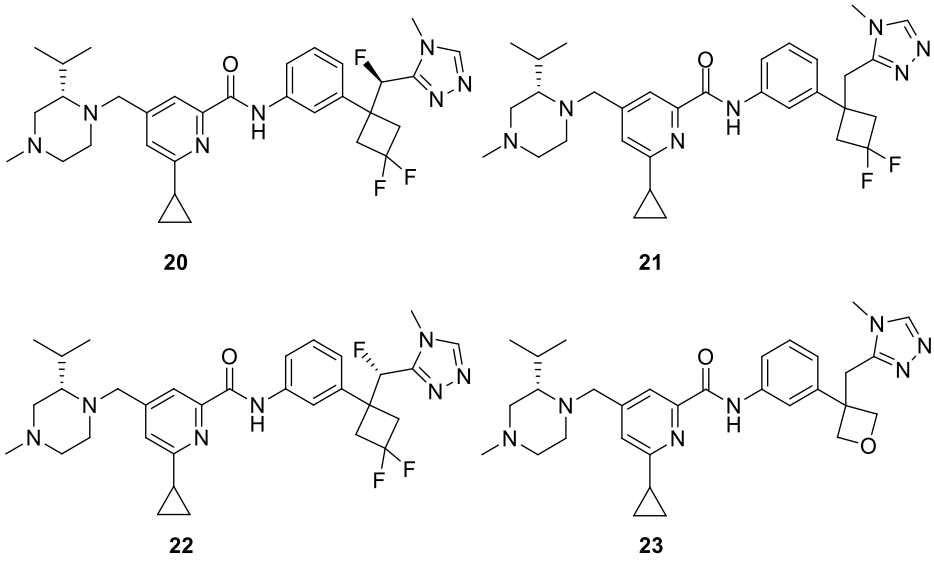

20 **21**

22 **23**

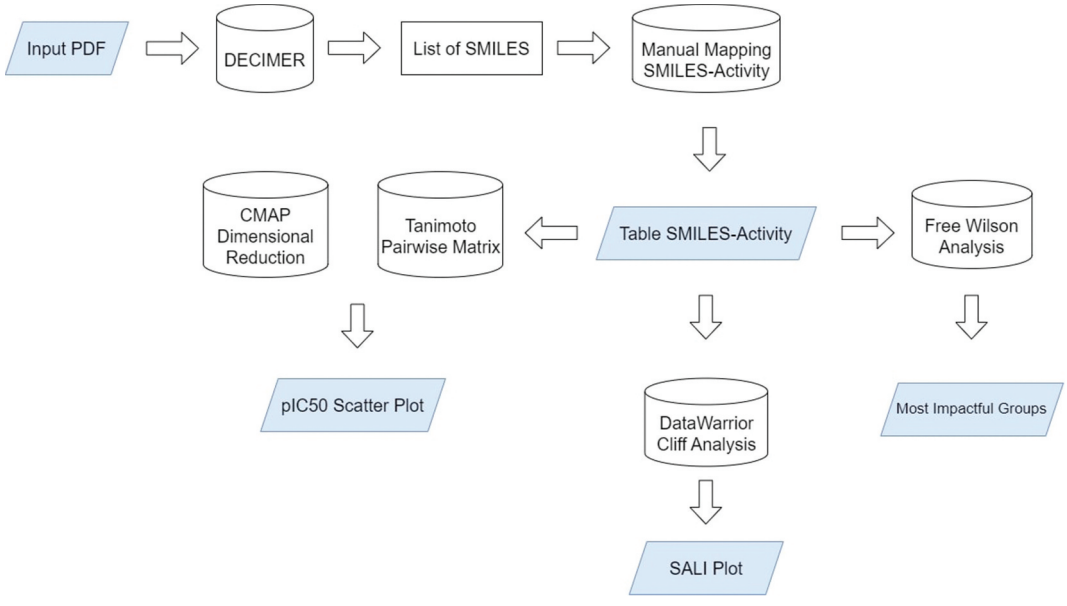

Figure 3. Structure of the in-house developed pipeline for high-throughput patent processing. At first DECIMER extract SMILES from the PDF document; the molecular activities are then assigned manually. Free Wilson analysis in than performed on the resulted table same table is further used for computing tanimoto pairwise matrix and dimensionally reduced through CMAP (in house python script used). Open Source DataWarrior software was used to perform cliff analysis that obtains a SALI (structure-Activity Landscape Index) plot.

and a combination of the central aromatic ring (benzene or pyridine) with R2 (typically a hydrophilic alkylamine substituent).

The first structure (General structure 7) contains a sequence of oxetane connected to a triazole moiety by a small methyl bridge. The R_1 part of the molecule typically consists of polar hydrophilic groups, such as piperidine or ethylene glycol. The molecules like 38, with hydrogen at the exact location already exhibits good activity in 300–1000 nM range. Most disclosed structures contain the trifluoromethyl group in position R1 (39). Substituting the R_2 moiety with methyl (40), difluoromethyl (41), or aldehyde (42) decreases the IC_{50} of the compound, with the latter substitution significantly reduces the activity range to 3000–10,000 nM compared to 300–1000 nM of 39. The activity of the following structure can be further enhanced by adding an amine group, reducing the IC_{50} range from 300–1000 nM to less than 100 nM. With the right combination of amine and alkyl substituents, chlorine substitution on R1 can be tolerated, resulting in compound 43 with an activity below 100 nM. Moreover, the binding pocket can tolerate a wide range of these polar substituents, as demonstrated by the activities of the substructures 44–46.

A second characteristic substructure of the HotSpot patent features an aromatic ring conjugated to the methyl stereocenter connected to a cyclobutyl moiety and a triazole compound. The molecule's stereochemistry is particularly important, as demonstrated by the compounds 47 and 48. The IC_{50} of the S isomer 47 is lower than 100 nM, while the R isomer 48 is a few orders of magnitude less potent, rendering it virtually inactive. In addition, the IC_{50} of structure 49 is more active than 38 (<200 nM vs 300–1000 nM), indicating better promise behind the following substructure type. Interestingly, the addition of hydrophilic amine moieties reverses the preference from S isomer to R isomer, as evidenced by the activity of the 49 and 50. Few substitutions are also tolerated at the cyclopropyl moiety. Addition of the methoxy group to compound 51 results in the compound 52 with similar activity range lower than 100 nM. However, introducing 2 fluorine atoms decreases the activity of the compound 53 to a higher activity range (300–1000 nM).

2.4. Nimbus

Nimbus Therapeutics has disclosed two patents featuring Cbl-b inhibitors. In 2022, the company reported Cbl-b compound NTX-801 (structure not disclosed) in the preclinical trial phase [25,26].

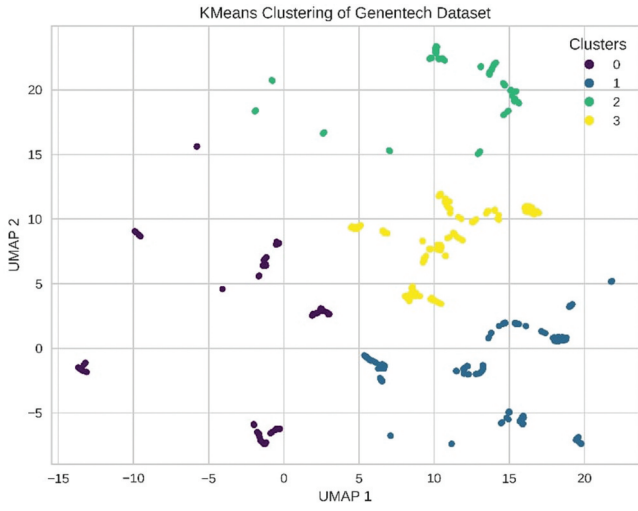

Figure 4. Pairwise tanimoto similarity matrix utilizing ECFP Morgan fingerprinting, followed by CMAP dimensional reduction and K-Means clustering. Each data point represents a molecule, and the relative distance represents the similarity.

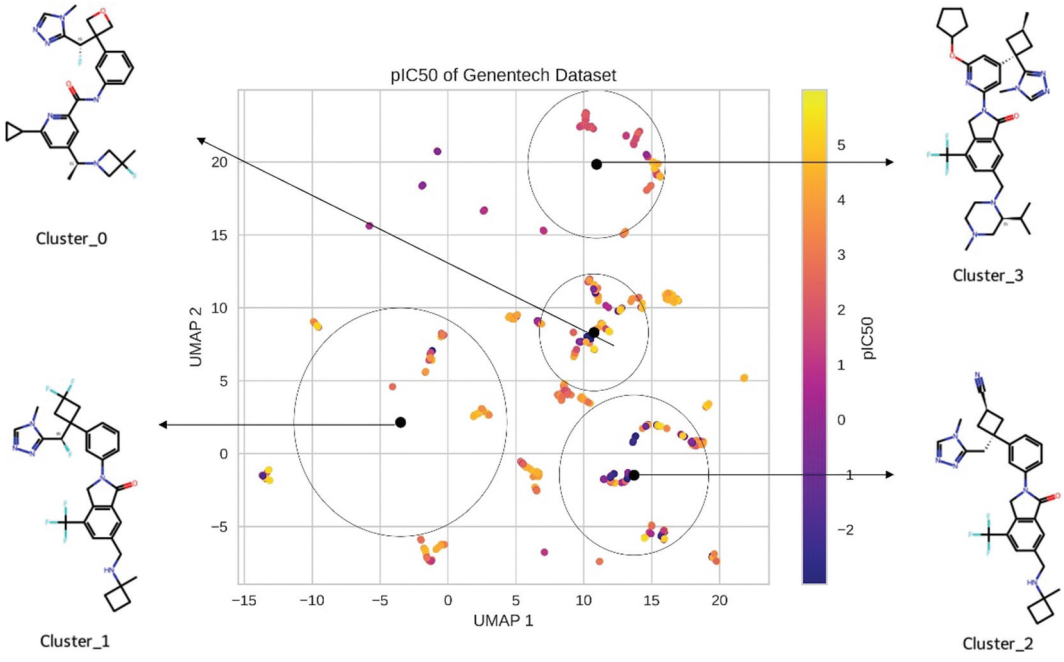

Figure 5. Pairwise tanimoto similarity matrix using ECFP Morgan fingerprinting, followed by CMAP dimensional reduction and K-Means clustering. Each data point represents a molecule, with the hue indicating the pIC_{50}. The cluster centroids are shown as black dots.

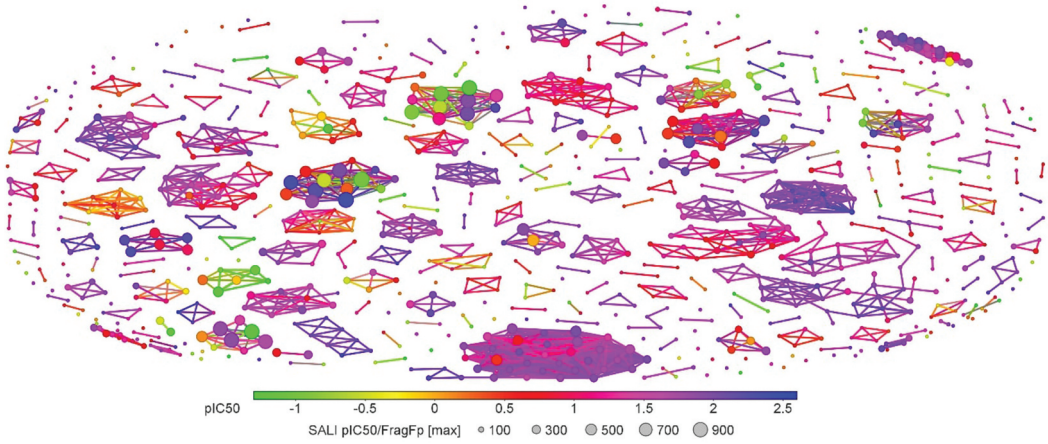

Figure 6. SALI plot of Genentech compounds. Each datapoint represents a molecule, and the relative distance among the datapoints represents the similarity based on Tanimoto similarity through ECFP fingerprints. The hue represents the pIC_{50}.

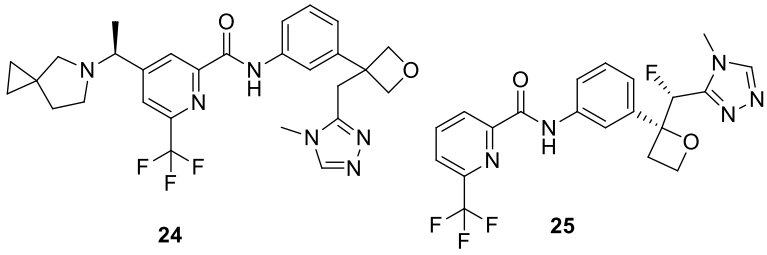

No updates have been disclosed since then, and the list of the companies pipeline does not feature Cbl-b anymore.

The first patent describes a set of molecules with benzazole core linked to a 6-membered (hetero)aromatic moiety acting as a bridge to a triazole ring (General Structure 8) [25]. Their binding affinities to Cbl-b were measured by TR-FRET and disclosed as IC_{50} ranges. In some compounds, the triazole may be replaced by diazole or tetrazole.

This substructure can tolerate various substituents at the hydrophilic moiety at R_1 and aromatic substituents R_2, R_3, and R_4. Some exemplary compounds, 54 and 55, have TR-FRET activities below 200 nM, Jurkat T-Cell assay activities below 200 nM, and AlphaLisa activities less than 1 µM.

The second Nimbus patent features the iso-oxindole substructure that acts as a linker between the pharmacophores similar to the one disclosed in the previous patent. [26] Most of the disclosed compounds inhibited the Cbl-b activity with IC_{50} values ≤200 nM, tested by RT-FRET. For example, 56 is very active in all the performed assays, including IC_{50} of TR-FRET activities in below 200 nM, EC_{50} of Jurkat T-Cell assay activities below 200 nM and AlphaLisa activities less than 1 µM.

2.5. Simcere

The Chinese company Simcere has published two patents on small-molecule inhibitors for Cbl-b [27,28]. The first patent highlights a series of 94 substituted naphthalactones (General Structure 9) [27]. This motif serves as a bridging link between an amine moiety and a combination of aromatic, cyclopropyl, and tetrazole moieties. Activities of the 14 most potent compounds were also disclosed, specifically as IC_{50} values from ubiquitination assay based on HTRF, which ranged from 16.5 nM to 107.5 nM. Additionally, five of these compounds were tested in the Jurkat T-cell assay, yielding EC_{50} values in the range of 264–616 nM. Compound SIM94 stands out with the lowest IC_{50} of 16 nM and an EC_{50} of 355 nM. in the Jurkat assay. Compound 57 has a slightly higher IC_{50} of 25.3 compared to 58, but it demonstrates more significant activity in the Jurkat assay, with a low EC_{50} of 264 nM.

The second patent by Simcere, filed in 2023, involves the General Structure 10 where a chromone is connected through an m-phenyl linker to R3. R3 consists of a substituted carbon linked to a 4-membered triazole moiety [28]. The compounds showed activity for inhibition of Cbl-b with IC_{50} values of 5 nM

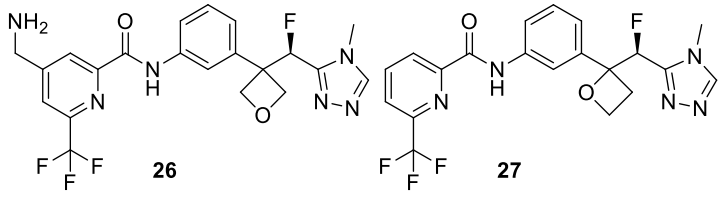

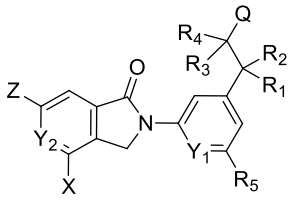

General Structure 5

2.6. Orum therapeutics

In 2023, Orum Therapeutics has disclosed a patent featuring antibody conjugates with small-molecule Cbl-b inhibitors [29]. Orum scientists investigated in vitro and in vivo biological activity of the Cbl-b inhibitor compounds in conjugation with anti-PD-1, anti CD7 and anti-CD25 antibodies. The General Structure 11 of the compounds involves a pyridine-oxindole core that binds an alkyl-tetrazole fragment with the amine moiety. Contrasting with other molecules discussed

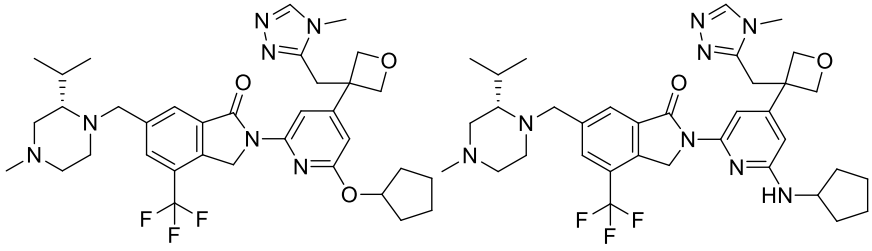

28 29

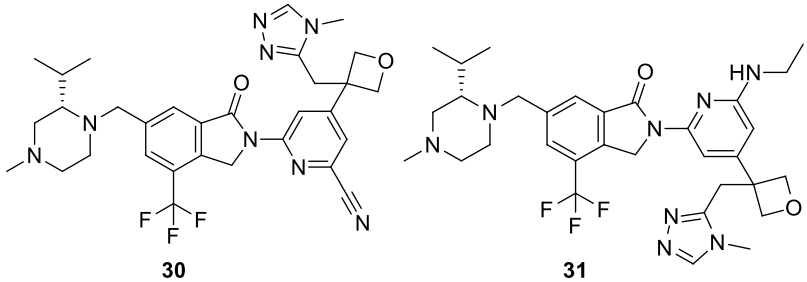

30 31

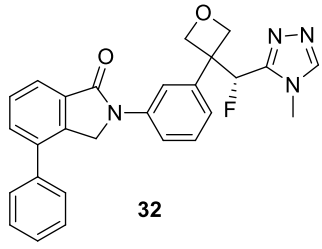

32

to 450 nM, assessed in the ubiquitination assay based on HTRF assay. The activities of 16 compounds for activating an IL-2 secretion in Jurkat T-cells were also disclosed, resulting in EC_{50} values ranging from 53 nM to 688 nM. Among the molecules presented, the 59 was the most active with the smallest IC_{50} for Ubiquitination and EC_{50} in Jurkat T cell assay, 5.4 nM and 53.6 nM, respectively.

above, these molecules contain an extra secondary amine on the pyridine that can be modified with a linker for the antibody conjugation. Although the individuals IC_{50} of these molecules were not disclosed, the T-Cell activation data in seven different cell lines for three small-molecule compounds 60–62 was shown. Compound 63 is an example of compound 61 with a linker for antibody conjugation.

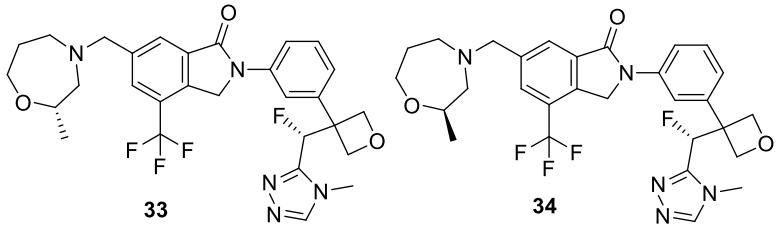

33 34

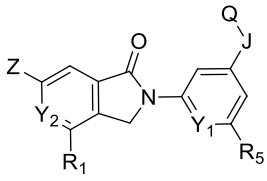

General Structure 6

2.7. InSilico design

InSilico Design has filed a Cbl-b related patent in 2023, that was made available publicly in January 2024 [30]. It features compounds with General Structure 12 and General Structure 13. The binding affinity of these compounds was measured by the HRTF assay and disclosed as concentration ranges – some exemplary compounds with IC_{50} <20 nM 64 and 65 are shown below.

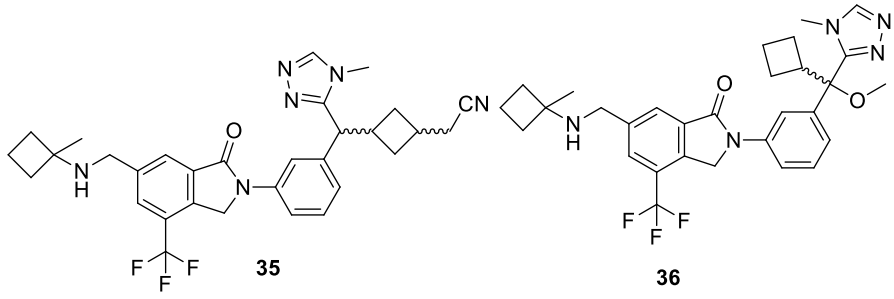

35

36

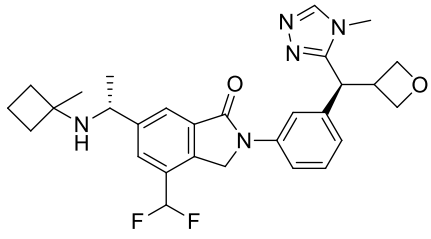

37

2.8. Arcus biosciences

Arcus Biosciences has filed a Cbl-b-related patent in 2023, that was published in January 2024. [26] The general structure 14 features a pyrollopyridinone core with some variability of substituents, connecting an ensemble of benzyl rings, alkyl moiety, and tetrazole substitutes with the hydrophilic part of the molecule. The compounds' affinity for Cbl-b and their effect on IL-2 secretion were assessed using HTRF and AlphaLISA assays, respectively, with data presented as concentration ranges. This resulted in IC_{50} and EC_{50} values in the range of less than 100 nM to up to 5 µM. For example, compound 66 showed potent binding with IC_{50} and EC_{50} values of less than 100 nM.

3. Expert opinion

Cbl-b is a new frontier in cancer drug discovery and development. It promises to revolutionize treatment by targeting the immune system's intricate controls, potentially offering a more precise and potent attack on cancer cells compared to traditional methods. Unlike therapies focusing solely on PD-1/PD-L1 pathways, which primarily lift the 'brakes' on immune cells, CBL-B inhibition could amplify the immune response more broadly, offering a dual advantage of enhancing cell-killing capabilities while potentially reducing the risk of resistance and improving outcomes across a wider range of cancers. This innovative approach embodies the next leap forward in immuno-oncology, aiming to outsmart cancer's cunning defenses with unmatched precision. In the highly dynamic landscape of Cbl-b research, the last few years have witnessed remarkable progress in patent disclosures, displaying a plethora of compounds by various companies. The intricate dance of two totally opposite fragments of the molecule: hydrophobic and hydrophilic are united by the greasy trifluoromethylated scaffold to create an assemble of pharmacophoric interactions.

After analyzing the molecules disclosed in the patents, we can speculate on some aspects of the Structure–Activity Relationship

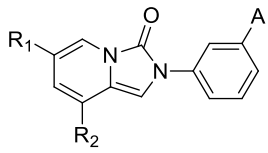

General Structure 7

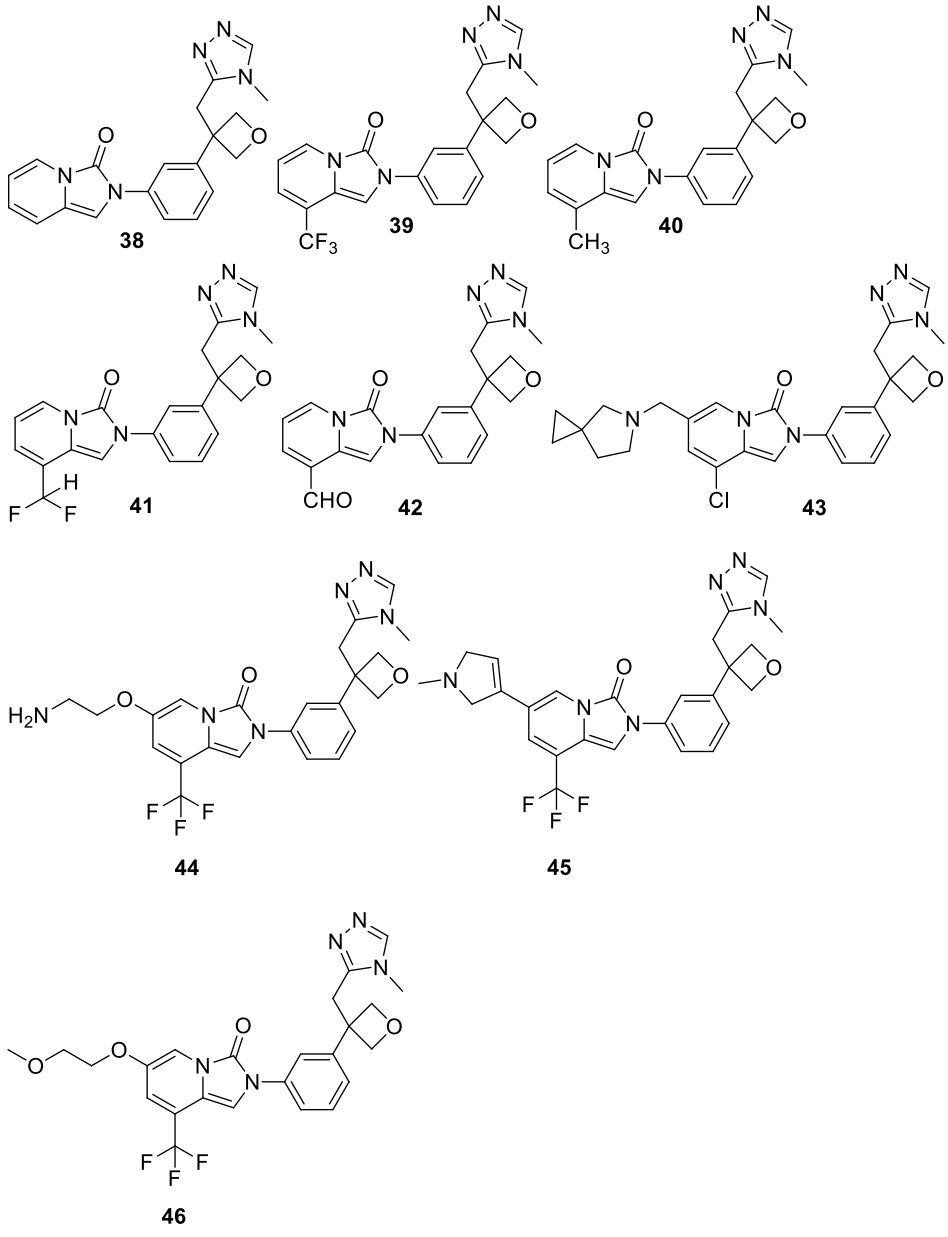

(SAR). Most structures, across various patents, display remarkably similar characteristics (General Structure 15). A Hydrogen Bond Donor (HBD) is crucial for targeting the backbone of Phe263 carbonyl (Figure 2(e)) with a hydrogen bond; numerous compounds achieve this through either a benzyl amide or a benzyl lactam, as seen in many structures from Nurix and Genentech. Another significant substitution at R1, widely represented in all patents, is a trifluoromethyl group that targets a greasy subpocket defined by the apolar side chain of Lys145, Arg141, and the backbone of Thr144.

This scaffold acts as a bridge between two separate substructures. Substructure A, which explores a wide range of moieties, targets a subpocket (see Figure 2(d)) capable of accommodating various moieties without compromising activity (so-called 'discontinuous' SAR since chemically different substituents do not widely impact the activity). This allows for a diverse array of chemical substituents. It is believed to be in a rather solvent-accessible area of the receptor, highlighting its potential in pharmacokinetic applications. Despite the variety of substituents presented by different companies, a consistent trend is observed: compounds with the appropriate stereochemistry for interacting with a subpocket, composed of Glu258, Glu268, and Pro72, show increased activity. It is notable that several compounds disclosed by various companies feature a piperidine-like substitution on the A portion. This suggests that the enhanced activity occurs due to hydrogen bond formation with Glu268.

Substructure B of the molecule is crucial for the activity and follows the principles of a 'continuous' Structure–Activity Relationship (SAR) [31], meaning that small changes can critically impact the activity cliff. It interacts with a critical Y-shaped subpocket (Figure 2(f)). Numerous compounds featuring a spiro substituent have been identified, whether modified on the 3' carbon or not. These compounds are linked to an aromatic 5-member ring, typically a triazole. The triazole occupies one side of the Y-shaped subpocket and engages in pi-stacking with Tyr363, while the spiro substituent fills the

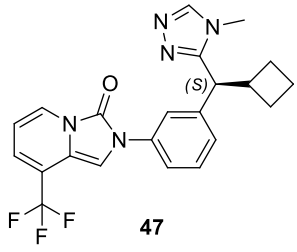

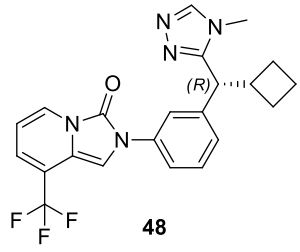

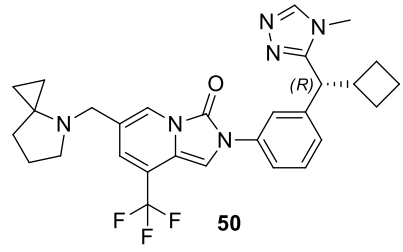

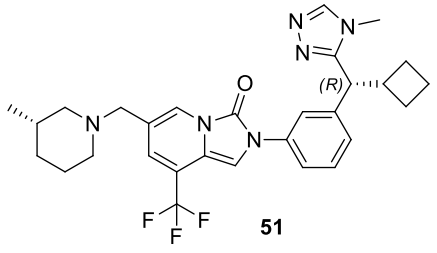

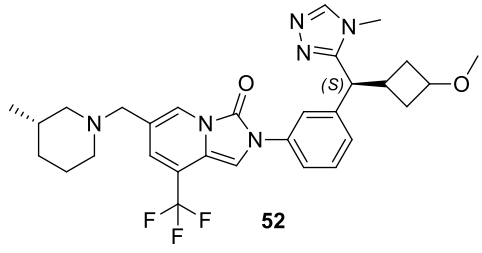

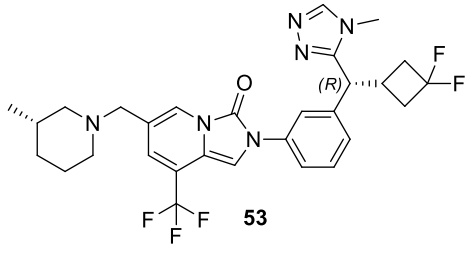

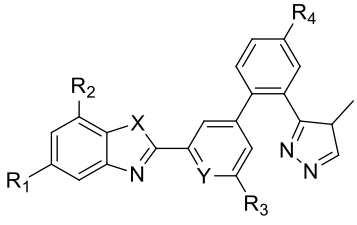

General Structure 8

other side. A cluster of water molecules around the Tyr363 is common among the different crystal structures, and since the triazole moiety is also common among the molecules within the patents, we might speculate that the presence of a water bridge stabilizes the triazole moiety in this pocket. A direct fit into the Y-shaped subpocket is essential as demonstrated by the poor activity of larger substituents such as 5-member ring (compound 6).

Overall, the well-characterized structure of the target protein and biological pathways allow for a precise identification of key pharmacophoric interaction, this leading to efficient structure-based discovery pipeline. In fact, based on the disclosed

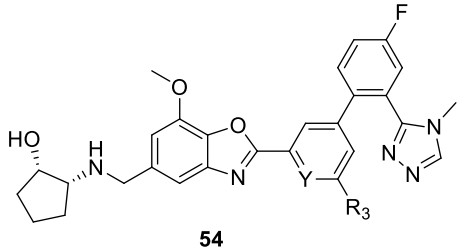

54

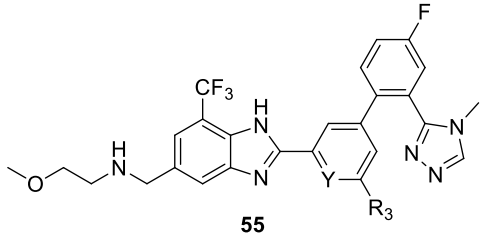

55

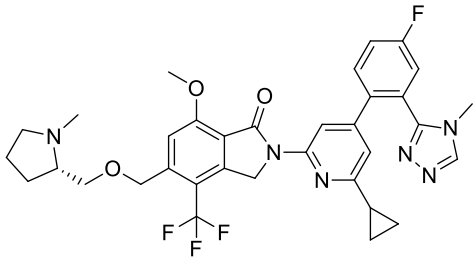

56

4. Chemoinformatic workflow

Patent information plays a crucial and supplementary role alongside published scientific literature, harboring key insights often obscured by the proprietary and economically valuable nature of drug discovery and development. The inherent complexity and guarded content within patents make them challenging to decipher, rendering patent analysis a labor-intensive task that typically requires expert intervention. Additionally, the vast amount of data contained in patents is not readily accessible through mere visual inspection. To address these challenges, we introduce a chemoinformatic pipeline designed to streamline and expedite the analysis of patent data. For this, we have implemented a straightforward, yet effective cheminformatics protocol to address this complexity to aid visual analysis (Figure 3). This protocol consists of a Deep Learning component capable of mining and converting the structure drawings into Simplified Molecular Input Line Entry System (SMILES) and a more traditional cheminformatics analysis that can decipher the covariance in R groups. We emphasize that certain types of cheminformatics analysis play a vital role in patent analysis due to the increasing quantity and complexity of such documents, helping avoid biases.

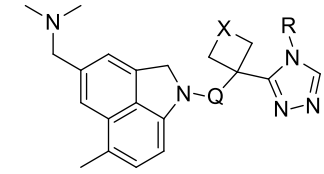

General Structure 9

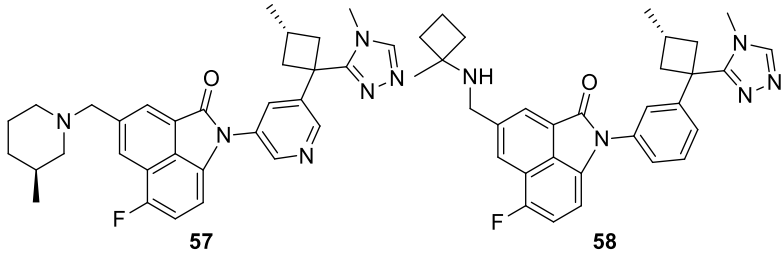

57 58

structures and activities, we can see that it is easy to engineer molecules that performs well in pre-clinical studies. Nevertheless, the good performance in pre-clinical trials does not guarantee successful clinical trials and subsequent adoption of the drug into clinical practice. Out of several analyzed companies, only Nurix and HotSpot are doing clinical trials. It is our opinion that the outcome of these clinical trials will both determine the viability of Cbl-b as a target in immunooncology and confirm that positive in-vitro data transfers into the patient outcome. Therefore, the success of these ongoing trials might encourage other companies to initiate their own clinical trials.

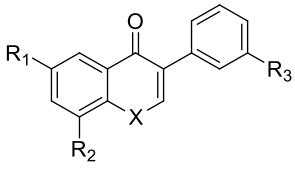

General Structure 10

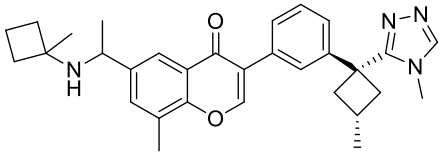

59

4.1. Structure mining

To better understand the diversity in structure and activity of entities described in patents, we chose Genentech's patent structures as our case study. This decision was based on Genentech providing specific IC_{50} values, unlike other companies offering only a range of values. Nonetheless, it is important to highlight that our overall pipeline also remains applicable to patents that offer activity data in ranges, not just precise values. The first step involves extracting structures from patents while ensuring the exclusion of any other graphical images; then, it is necessary to convert these structures into SMILES representation for inclusion in a cheminformatics workflow.

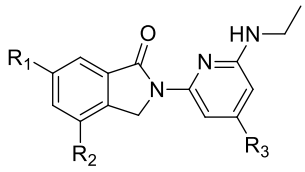

General Structure 11

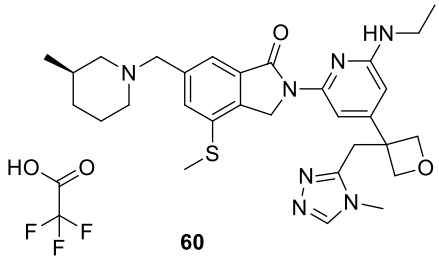

60

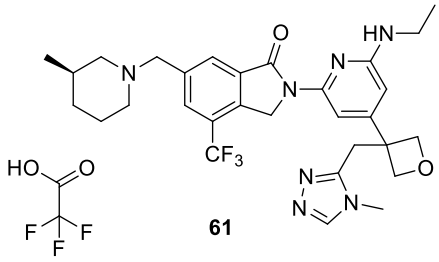

61

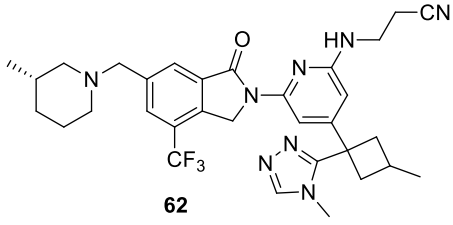

62

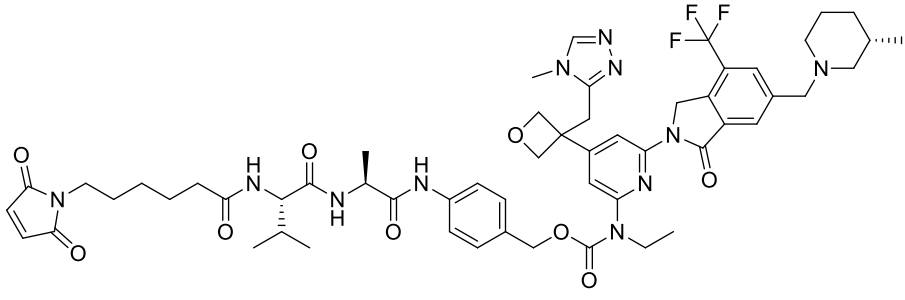

63

The Optical Chemical Structure Recognition (OCSR) tool, DECIMER, can perform the listed operations into a single workflow, taking as input just the pages/scans containing the drawing of the structures [32]. DECIMER is not capable of extracting IC_{50} values and associating them with SMILES, so we manually conducted this operation. This resulted in a table containing the molecule name, the SMILES, and the activity ready for an exploratory chemoinformatic analysis.

4.2. Free Wilson Analysis

Free Wilson Analysis is a method utilized to understand substituents' impact on activity [33]. This approach involves constructing a matrix with rows corresponding to compounds and columns reflecting the presence or absence of each substituent. Regression analysis is then performed on this matrix, yielding coefficients for each substituent that indicate their contribution to the molecule's activity. This analysis is most effective when the dataset has a diverse range of single substituent combinations, enabling more accurate inferences from regression-based machine learning. In the test dataset from Genentech, not all compounds met this criterion. However, combining this type of analysis with a simple SMART pattern search can effectively identify molecules with single substituent modifications, thereby facilitating a better comparison of their activities.

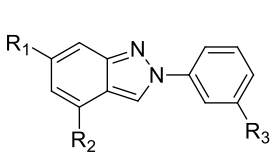

General Structure 12

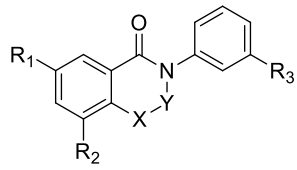

General Structure 13

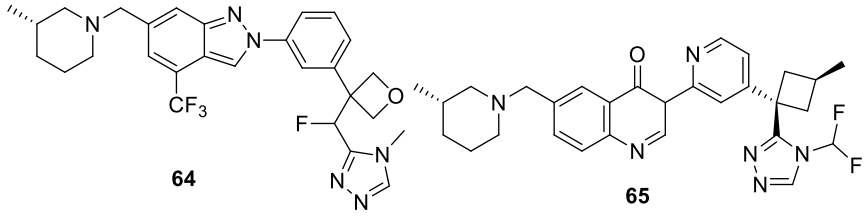

64 65

4.3. CMAP Analysis

The first type of information crucial for rationalizing the SAR is understanding whether the SARs are 'continuous' or 'discontinuous' [31]. In the first case, minor structural modifications can dramatically affect the activity (activity cliff), while chemically diverse compounds exhibit the same activity in the second case. One type of SAR does not exclude the other, and both these antithetic behaviors can rationalize the same pocket; this is possible because the 3D similarity can be vastly different from the 2D similarity.

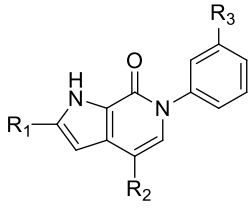

General Structure 14

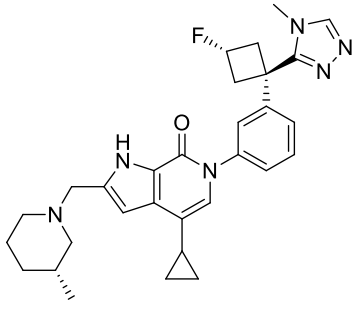

66

So, to rationalize this behavior, the following operations on the dataset were performed through an in-house Python script (1) The similarity of all the compounds was assessed using the Tanimoto Similarity Score (TSS), resulting in a 2D matrix of similarity, (2) The Tanimoto similarity matrix was then subjected to CMAP dimensionality reduction. This step transforms the high-dimensional similarity data into a more manageable, lower-dimensional format; (3) Following the CMAP dimensionality reduction, KMeans clustering was performed, grouping compounds into distinct clusters based on their similarity (Figures 4–5). Each dot in the resulting scatterplot was colored based on the pIC_{50}, revealing the general behavior of the molecules. Active molecules were found in all clusters, suggesting that the Structure–Activity Relationship (SAR) would exhibit a 'discontinuous' behavior. However, not surprisingly, many non-potent molecules were also found in clusters predominantly occupied by active molecules, suggesting a 'continuous' behavior. This analysis helped us identify clusters of distinct structures with similar activities for patents analyzed above.

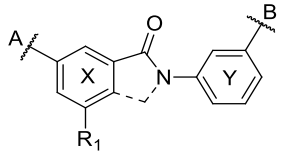

4.4. Activity cliff analysis

To improve our understanding of substituent interaction, we conducted a Cliff Analysis through the chemoinformatic tool DataWarrior [34]. It computes the Tanimoto Similarity Matrix and a dimensionality reduction, then examines pairs of similar structures below a customizable cutoff and calculates the difference in activity (pIC_{50}, pKd) relative to their dissimilarity. This analysis produces a Structure-Activity Landscape Index (SALI) plot (Figure 6), offering insights into the significance of changes in molecular activity compared to their structural variations.

Funding

This paper was funded by the ERA Chair grant ACCELERATOR (101087318) and the ERC Advanced grant AMADEUS (101098001). This study was supported (to AD) by the National Institute for Cancer Research—Programme EXCELES (ID Project No. LX22NPO5102), and the Dutch Cancer Society (KWF Kankerbestrijding, KWF) grant (14712).

Declaration of interest

The authors have no relevant affiliations or financial involvement with any organization or entity with a financial interest in or financial conflict with the subject matter or materials discussed in the manuscript. This includes employment, consultancies, honoraria, stock ownership or options, expert testimony, grants or patents received or pending, or royalties.

Reviewer disclosures

Peer reviewers on this manuscript have no relevant financial or other relationships to disclose.

Author contribution statement

R.D, Z.S, I.C and A.L. wrote the manuscript with and under the supervision of A.D.

ORCID

Alexander Dömling http://orcid.org/0000-0002-9923-8873

References

Papers of special note have been highlighted as either of interest (•) or of considerable interest (••) to readers.

1. Liu Q, Zhou H, Langdon WY, et al. E3 ubiquitin ligase Cbl-b in innate and adaptive immunity. Cell Cycle. 2014;13(12):1875–1884. doi: 10.4161/cc.29213
2. Tang R, Langdon WY, Zhang J. Regulation of immune responses by E3 ubiquitin ligase cbl-b. Cell Immunol. 2019 Jun;340:103878. doi: 10.1016/j.cellimm.2018.11.002
3. Paolino M, Penninger JM. Cbl-b in T-cell activation. Semin Immunopathol. 2010 Jun;32(2):137–148. doi: 10.1007/s00281-010-0197-9
4. Wallner S, Gruber T, Baier G, et al. Releasing the brake: targeting Cbl-b to enhance lymphocyte effector functions. Clin Dev Immunol. 2012;2012:1–5. doi: 10.1155/2012/692639
5. Augustin RC, Bao R, Luke JJ. Targeting cbl-b in cancer immunotherapy. J Immunother Cancer. 2023;11(2):e006007. doi: 10.1136/jitc-2022-006007

•• **of considerable interest.**

6. Chiang JY, Jang IK, Hodes R, et al. Ablation of Cbl-b provides protection against transplanted and spontaneous tumors. J Clin Invest. 2007 Apr;117(4):1029–1036. doi: 10.1172/JCI29472

•• **of considerable interest.**

7. Loeser S, Loser K, Bijker MS, et al. Spontaneous tumor rejection by cbl-b –deficient CD8+ T cells. J Expir Med. 2007 Apr 16;204 (4):879–891. doi: 10.1084/jem.20061699
8. Paolino M, Thien CB, Gruber T, et al. Essential role of E3 ubiquitin ligase activity in cbl-b– regulated T cell functions. J Immunol. 2011 Feb 15;186(4):2138–2147. doi: 10.4049/jimmunol.1003390

•• **of considerable interest.**

9. Jafari D, Mousavi MJ, Keshavarz Shahbaz S, et al. E3 ubiquitin ligase casitas B lineage lymphoma-b and its potential therapeutic implications for immunotherapy. Clin Exp Immunol. 2021 Apr;204 (1):14–31. doi: 10.1111/cei.13560
10. Zhou L, Yang J, Zhang K, et al. Rising star in immunotherapy: development and therapeutic potential of small-molecule inhibitors targeting casitas B cell lymphoma-b (cbl-b). J Med Chem. 2024 Jan 25;67(2):816–837. doi: 10.1021/acs.jmedchem.3c01361

•• **of considerable interest.**

11. Meng W, Sawasdikosol S, Burakoff SJ, et al. Structure of the amino-terminal domain of cbl complexed to its binding site on ZAP-70 kinase. Nature. 1999 Mar 4;398(6722):84–90. doi: 10.1038/18050

•• **of considerable interest.**

12. Levkowitz G, Waterman H, Ettenberg SA, et al. Ubiquitin ligase activity and tyrosine phosphorylation underlie suppression of growth factor signaling by c-Cbl/Sli-1. Mol Cell. 1999 Dec;4 (6):1029–1040. doi: 10.1016/S1097-2765(00)80231-2
13. Abe T, Hirasaka K, Nikawa T. Involvement of cbl-b-mediated macrophage inactivation in insulin resistance. World J Diabetes. 2017 Mar 15;8(3):97–103. doi: 10.4239/wjd.v8.i3.97
14. Kobashigawa Y, Tomitaka A, Kumeta H, et al. Autoinhibition and phosphorylation-induced activation mechanisms of human cancer and autoimmune disease-related E3 protein cbl-b. Proc Natl Acad Sci U S A. 2011 Dec 20;108(51):20579–20584. doi: 10.1073/pnas.1110712108
15. Dou H, Buetow L, Sibbet GJ, et al. Essentiality of a non-ring element in priming donor ubiquitin for catalysis by a monomeric E3. Nat Struct Mol Biol. 2013 Aug;20(8):982–986. doi: 10.1038/nsmb.2621

•• **of considerable interest.**

16. Barsanti P, Bence NF, Gosling J, et al. inventors; Nurix Therapeutics Inc. assignee. Inhibitors of cbl-B and Methods of use thereof patent WO2019148005A1. 2019 Aug 01.

•• **of considerable interest.**

17. Sands AT, Bence NF, Zapf CW, et al. inventors; Nurix Therapeutics Inc. assignee. 3-substituted piperidine compounds for cbl-B inhibition. And use of a Cbl-B inhibitor in combination with a cancer vaccine and/or oncolytic virus patent WO2020210508A1. 2020 Oct 15.

•• **of considerable interest.**

18. Sands A, Bence NF, Zapf CW, et al., inventors; Nurix therapeutics Inc, assignee. Cyano Cyclobutyl Compd For Cbl-B Inhib And Uses Thereof Patent CA3140873A1. 2020 Nov 26.

•• **of considerable interest.**

19. Sands AT, Bence NF, Zapf CW, et al. inventors; Nurix Therapeutics Inc. assignee. Substituted benzyl-triazole compounds for cbl-B inhibition, and further uses thereof patent WO2020264398A1. 2020 Dec 30.

•• **of considerable interest.**

20. Sands AT, Bence NF, Zapf CW, et al. inventors; Nurix Therapeutics Inc. assignee. Urea, amide, and substituted heteroaryl compounds for cbl-B inhibition patent WO2021021761A1. 2021 Feb 04.

•• **of considerable interest.**

21. Liang J, Jakalian A, Lambrecht MJ, et al. inventors; Genentech Inc. assignee. Amides as cbl-B inhibitors patent WO2022169998A1. 2022 Aug 11.

•• **of considerable interest.**

22. Liang J, Jakalian A, Lambrecht MJ, et al. inventors; Genentech Inc. assignee. Lactams as cbl-B inhibitors patent WO2022169997A1. 2022 Aug 11.

•• **of considerable interest.**

23. Huestis M, Lambrecht MJ, Liang J, et al. inventors; Genentech Inc. assignee. Lactams as cbl-B inhibitors selective over C-Cbl patent WO2023081853A1. 2023 May 11.

•• **of considerable interest.**

24. Bi Y, Carson K, Harriman GC, et al., inventors; Hotspot therapeutics Inc, assignee. Compounds, compositions and methods of treating cancer patent WO2022221704A1. 2022 Oct 20.

•• **of considerable interest.**

25. Leit DMSM, West AV, Baker T, et al. inventors; Nimbus Clio Inc. assignee. Cbl-B modulators and uses thereof patent WO2022217276A1. 2022 Oct 13.

•• **of considerable interest.**

26. Leit DMSM, West AV, Baker T, et al. inventors; Nimbus Clio Inc. assignee. Cbl-B modulators and uses thereof patent WO2022272248A1. 2022 Dec 29.

•• **of considerable interest.**

27. Mai W, Liu X, Zhu W, et al., inventors; Simcere zaiming pharmaceutical Co ltd, assignee. Tricyclic compound as cbl-B inhibitor patent WO2023036330A1. 2023 Mar 16.

•• **of considerable interest.**

28. Mai W, Liu X, Shi W, et al., inventors; Simcere zaiming pharmaceutical Co ltd, assignee. Polycyclic compound as cbl-B inhibitor patent WO2023072273A1. 2023 May 04.

•• **of considerable interest.**

29. Park PU, Fishkin N, Bai C, et al. inventors; Orum Therapeutics Inc. assignee. Activators of effector T cells patent WO2023170608A1. 2023 Sep 14.

•• **of considerable interest.**

30. Ding X, Liu X, Liu Y, et al., inventors; Insilico medicine ip ltd, assignee. Cbl-B inhibitors and methods of uses thereof patent WO2024017201A1. 2024 Jan 25.

•• **of considerable interest.**

31. Bajorath J, Peltason L, Wawer M, et al. Navigating structure–activity landscapes. Drug Discovery Today. 2009 Jul;14(13–14):698–705. doi: 10.1016/j.drudis.2009.04.003
• **of interest.**
32. Rajan K, Brinkhaus HO, Agea MI, et al. Decimer.ai: an open platform for automated optical chemical structure identification, segmentation and recognition in scientific publications. Nat Commun. 2023 Aug 19;14(1):5045. doi: 10.1038/s41467-023-40782-0
33. Kubinyi H. Free Wilson Analysis. Theory, applications and its relationship to Hansch Analysis. Quant Struct-Act Relat. 2006;7 (3):121–133. doi: 10.1002/qsar.19880070303
34. Sander T, Freyss J, von Korff M, et al. DataWarrior: an open-source program for chemistry aware data visualization and analysis. J Chem Inf Model. 2015 Feb 23;55(2):460–473. doi: 10.1021/ci500588j
• **of interest.**